Molecular Neurobiology (2018) 55:7164–7178
https://doi.org/10.1007/s12035-018-0901-7

A Fragment of Adhesion Molecule L1 Binds to Nuclear Receptors to Regulate Synaptic Plasticity and Motor Coordination

Kristina Kraus[1] · Ralf Kleene[1] · Melad Henis[2,3] · Ingke Braren[4] · Hardeep Kataria[1] · Ahmed Sharaf[2,5] · Gabriele Loers[1] · Melitta Schachner[6,7] · David Lutz[1,2]

Received: 6 September 2017 / Accepted: 10 January 2018 / Published online: 30 January 2018

Abstract

Proteolytic cleavage of the neuronal isoform of the murine cell adhesion molecule L1, triggered by stimulation of the cognate L1-dependent signaling pathways, results in the generation and nuclear import of an L1 fragment that contains the intracellular domain, the transmembrane domain, and part of the extracellular domain. Here, we show that the LXXLL and FXXLF motifs in the extracellular and transmembrane domain of this L1 fragment mediate the interaction with the nuclear estrogen receptors α (ERα) and β (ERβ), peroxisome proliferator-activated receptor γ (PPARγ), and retinoid X receptor β (RXRβ). Mutations of the LXXLL motif in the transmembrane domain and of the FXXLF motif in the extracellular domain disturb the interaction of the L1 fragment with these nuclear receptors and, when introduced by viral transduction into mouse embryos in utero, result in impaired motor coordination, learning and memory, as well as synaptic connectivity in the cerebellum, in adulthood. These impairments are similar to those observed in the L1-deficient mouse. Our findings suggest that the interplay of nuclear L1 and distinct nuclear receptors is associated with synaptic contact formation and plasticity.

Keywords Cell adhesion molecule · L1CAM · Nuclear receptors · Motor coordination · Cerebellar circuitry · Synaptic plasticity

✉ Melitta Schachner
schachner@stu.edu.cn

✉ David Lutz
david.lutz@zmnh.uni-hamburg.de

[1] Arbeitsgruppe für Biosynthese Neuraler Strukturen, Universitätsklinikum Hamburg-Eppendorf, Martinistr. 52, 20246 Hamburg, Germany

[2] Institut für Strukturelle Neurobiologie, Universitätsklinikum Hamburg-Eppendorf, Martinistr. 52, 20246 Hamburg, Germany

[3] Department of Anatomy and Histology, Faculty of Veterinary Medicine, Assiut University, Assiut 71526, Egypt

[4] Vector Core Unit, Institut für Experimentelle Pharmakologie und Toxikologie, Universitätsklinikum Hamburg-Eppendorf, Martinistr. 52, 20246 Hamburg, Germany

[5] Department of Histology and Cytology, Faculty of Veterinary Medicine, Zagazig University, Zagazig 44519, Egypt

[6] Keck Center for Collaborative Neuroscience and Department of Cell Biology and Neuroscience, Rutgers University, 604 Allison Road, Piscataway, NJ 08854, USA

[7] Center for Neuroscience, Shantou University Medical College, 22 Xin Ling Road, Shantou, Guangdong 515041, China

Introduction

The cell adhesion molecule L1 plays important functional roles in the developing and adult nervous system by modulating a variety of morphogenic events involved in neuronal migration and survival, axonal outgrowth and fasciculation, myelination, synaptic plasticity, learning and memory, and regeneration after injury (for reviews, see [1–8]). In humans, a plethora of L1CAM gene mutations is associated with the L1 syndrome characterized by hydrocephalus, severe intellectual disability, aphasia, and motor dysfunctions, such as ataxia, paraplegia, and shuffling gate. In addition, L1 has been linked to other neural disorders, such as fetal alcohol syndrome, Hirschsprung's disease, schizophrenia, and Alzheimer's disease [5, 7, 9–14].

Many functions of L1 in the nervous system depend on regulated proteolytic cleavage [15–24]. In previous studies, we have shown that the stimulation of L1 signaling leads to the generation of a 70-kDa L1 fragment (L1-70) by the serine protease myelin basic protein, which cleaves L1 at Arg_{687} [25, 26]. A cleavage of this fragment at Glu_{1167} in the intracellular domain by cathepsin E yields a 30-kDa fragment [27]. Both fragments are imported into the cell nucleus and involved in regulating L1-dependent functions, such as neurite outgrowth,

neuronal cell migration, and survival, myelination by Schwann cells as well as Schwann cell proliferation, migration, and process formation [26–28]. In addition, L1-70 appears to play a role in neural differentiation, myelination, and synaptogenesis in the developing postnatal spinal cord, as well as functional recovery after injury and Alzheimer's disease [25, 28, 29].

The murine L1 contains an LXXLL motif (L_{1136}LILL) in the transmembrane domain and an FXXLF motif (F_{1046}HILF) in the fifth fibronectin type III repeat. The LXXLL motif has been found in co-activators and co-repressors of nuclear receptors (for review and references, see [30–32]). Nuclear receptors represent a superfamily of transcription factors and play important roles in eukaryotic development, differentiation, and metabolic homeostasis. They are subdivided into three classes. Class I includes members of the steroid receptor family, such as receptors for progesterone, estrogen, androgen, glucocorticoid, and mineralocorticoid. Class II includes members of the thyroid/retinoid family, such as the peroxisome proliferator-activated receptors and receptors for thyroid hormone, vitamin D, and retinoic acid. Class III comprises members of the orphan receptor family. The FXXLF motif shows similar structural features like the LXXLL motif and seems to be involved in the stabilization of ligand-bound nuclear receptors [33–37].

Since L1-70 contains the LXXLL and FXXLF motifs which mediate and affect the interaction of co-activators and co-repressors with nuclear receptors, we investigated whether these motifs are involved in the interaction with nuclear receptors. We show that nuclear receptors ERα and ERβ, PPARγ, and RXRβ interact with L1-70, and provide evidence that the lack of interaction of nuclear L1 with nuclear receptors is associated with malformation of synaptic contacts in the cerebellum and with dysfunctions in motor coordination and learning.

Materials and Methods

Animals

L1-deficient male mice [38] were maintained as heterozygous breeding pairs on a mixed genetic background (129SVJ × C57BL/6 × Black Swiss). Wild-type male littermates were used as controls. Mice were maintained under standard laboratory conditions with food and water supply ad libitum and with a 12-h light/dark cycle. All experiments were conducted in accordance with the German and European Community laws on protection of experimental animals, and all procedures used were approved by the responsible committee of The State of Hamburg (TVA 6/14, TVA 098/09). Experiments were carried out and the manuscript was prepared following the ARRIVE guidelines for animal research [39].

Antibodies and Reagents

Monoclonal L1 antibody 555 has been described [40]. Monoclonal mouse L1 antibody anti-CD171 (clone 74-5H7; cat no. 38101; lot: B222192) was from Biolegend (San Diego, CA, USA). Polyclonal rabbit L1 antibody anti-L1CAM (ab123990; lot: GR104917-13) and mouse GAD67 antibody (ab26116) were from Abcam (Cambridge, UK). Rabbit antibodies recognizing the androgen receptor (AR) (N-20; sc-816; lot: J1111), the vitamin D receptor (VDR) (C-20; sc-1008; lot: G2511), retinoid X receptors (RXR) (C-20; sc-831; lot: H1611), ERα (HC-20; sc-543; lot: G1513), and PPARγ (H-100; sc-7196; lot: E0611) were from Santa Cruz Biotechnology (Heidelberg, Germany). Mouse calbindin (C9848; lot: unknown) and rabbit calbindin (C2724; lot: unknown) antibodies were from Sigma-Aldrich (Taufkirchen, Germany). Normal donkey serum and secondary antibodies coupled to horseradish peroxidase (HRP) or to fluorescent dyes were from Dianova (Hamburg, Germany). The antibody against vGLUT-1 (vesicular glutamate transporter 1, BNPI, SLC17A7; lot: 135,311/30) was from Synaptic Systems (Göttingen, Germany).

Recombinant AR (AR-991H; GST-tag; full-length human AR), ERα (ESR1-12557H; GST-tag; amino acids 65-280 of human ERα), VDR (VDR-3659H; his-tag; amino acids 128-427 of human VDR), and PPARγ (PPARG-2772H; his-tag; amino acids 209-477 of human PPARγ) were from Creative Biomart (Shirley, NY, USA). Liver X receptor (LXR) (NR1H2; ABN-H00007376-P01-1, GST-tag; full-length human LXR) and ERβ (ESR2; ABN-H00002100-P01-2, GST-tag; full-length human ESR2) were from Abnova (Taipei City, Taiwan), and RXR (BML-SE127-0050; human RXRβ) was from Enzo Life Sciences (Lörrach, Germany). Recombinant proteins comprising the intracellular L1 or CHL1 domains were described [41].

Sequence Analysis

The L1 protein sequence was subjected to online database search for protein binding motifs using Minimotif Miner (http://minimotifminer.org or http://mnm.engr.uconn.edu). The identified motifs were applied to online screening using the ScanProsite tool of ExPASy Bioinformatics Resource Portal (http://prosite.expasy.org/scanprosite/) with filter settings "mammalia" for taxonomy and "neural cell adhesion" for description to identify similarities in other species and in other neural cell adhesion molecules. Hits were inspected for immunoglobulin family members.

Preparation of Nuclear Extracts

The isolation of nuclei and preparation of nuclear extracts from brains of 7-day-old mice has been described [25]. Briefly, brains were homogenized in homogenization buffer (0.32 M sucrose, 10 mM Tris/HCl, pH 7.4) and centrifuged at 1000×*g* and 4 °C for 10 min. The pellet was resuspended in homogenization buffer and applied to a gradient of 35%, 30% and 25% Optiprep (Axis Shield Diagnostics, Dundee, UK). After centrifugation at 10,000×g and 4 °C for 20 min, the nuclei-containing fraction was collected from the 30%/35% interphase, diluted and washed in homogenization buffer by centrifugation at 1000 g and 4 °C for 20 min. The nuclear pellet was resuspended in an extraction buffer (10 mM Hepes, 10 mM KCl, 2 mM $MgCl_2$, 500 mM NaCl, 25% glycerol, pH 7.5) with 1× protease inhibitor cocktail (Roche Diagnostics, Mannheim, Germany) and incubated on ice for 30 min. After centrifugation at 10,000 g and 4 °C for 5 min, the supernatant was taken as a nuclear extract.

For immunoblot analysis of the nuclear extract from transduced cerebellar granule cells, cells were pelleted at 3000×*g* and 4 °C for 5 min. The cell pellet was resuspended in lysis buffer (20 mM Tris/HCl, pH 7.4, 150 mM NaCl, 1 mM EDTA, 1 mM EGTA, 1% NP-40, 10 μM DTT, 25 U/ml benzonase, 1× protease inhibitor solution) and incubated on ice for 5 min. After centrifugation at 3000×*g* and 4 °C for 5 min, the pellet was resuspended in urea-containing lysis buffer (100 mM Tris/HCl, pH 7.4, 12 mM magnesium acetate tetra hydrate, 6 M urea, 2% SDS, 10 μM DTT, 25 U/ml benzonase, 1× protease inhibitor solution) and incubated on ice for 30 min. After centrifugation at 20,000×*g* for 10 min at 4 °C, the supernatant was taken as nuclear extract.

Nuclear extracts from transduced cerebellar granule cells for ELISA were prepared using the subcellular fractionation kit for cultured cells (ThermoFisher Scientific, Darmstadt, Germany) according to the manufacturer's instructions. The fractions containing soluble nuclear proteins or chromatin-bound proteins were pooled and used as a nuclear extract.

Immunoblot Analysis and Immunoprecipitation

Immunoblot analysis and immunoprecipitation were performed as described [42].

Site-Directed Mutagenesis of L1 and Production of AAVs

For site-directed mutagenesis of $_{1046}$FHILF into $_{1046}$YHIAY and of $_{1136}$LLILL into $_{1136}$ALIAA, the following primers and a vector coding for mouse L1 were used: fw 1046 (5'-AAG GGC CAG TGC AAT TTC AGG ***TAC*** CAT ATC ***GCGTAC*** AAA GCC TTA CCA GAA GGG AAA GTG-3') and rev 1046 (5'-TTT CCC TTC TGG TAA GGC TTT ***GTACGC*** GATATG ***GTA*** CCT GAA ATT GCA CTG GCC CTT CCG-3') or fw 1136 (5'-GTC AGC GCT ATC ATT CTC TTG ***GCG*** CTC ATC ***GCGGCG*** ATC CTC TGC TTC ATC AAA CGC AGC-3') and rev 1136 (5'-GCGTTTGA TGAAGCAGAGGAT ***CGCCGC*** GAT GAG ***CGC*** CAA GAG AAT GAT AGC GCT GAC AAA-3') (mutations are shown in bold and italic). Subcloning of wild-type and mutated L1 into a pAAV-MCS vector (CMV promoter; Cell Biolabs, San Diego, CA, USA) via a SalI restriction site was performed using the InFusion Cloning Kit (Clontech; Takara Bio, Mountain View, CA, USA), PCR amplification with Phusion Polymerase (New England Biolabs, Ipswich, MA, USA), and the following primers: fw (5'-A TCC TCT AGA GTC GAC **ATG GTC GTG ATG CTG CGG TAC**-3') and rev (5'-G CTT CTG CAG GTC GAC **CTA TTC TAG GGC TAC TGC AGG**-3) (the L1 sequence is shown in bold). Production of AAV1 coding for wild-type and mutated L1 was performed as described [26].

Preparation, Transduction, and Treatment of Cerebellar Neurons

Cerebellar neurons were prepared from 6- to 8-day-old mice as described [25, 42, 43]. For viral transduction, AAV1 carrying wild-type and mutant L1 were incubated at a 1000-fold multiplicity of infection with L1-deficient cerebellar neurons (2×10^6 cells/well) for 24 h. Cerebellar neurons were stimulated with 10 μg/ml L1-Fc for 2 h at 37 °C.

In Utero Injection of Viral Particles

In utero injection of 4×10^{12} empty AAV1 or AAV1 encoding wild-type L1 or mutated L1 into embryos at embryonic day 16 was performed as described [25].

Tissue Preparation, Immunohistochemistry, and Electron Microscopy

Tissue fixation and sectioning were performed as described [28]. Briefly, after perfusion of mice, brains were incubated in phosphate buffered saline, pH 7.3 (PBS) for 5 h under gentle agitation at room temperature. For dehydration, the tissue was first incubated in 70% ethanol overnight and then subjected to consecutive incubations in 80, 90, and 100% ethanol at room temperature for 1 h each. The tissue was incubated two times in xylene for 2 h and then in liquid paraffin wax at 62 °C overnight, followed by overnight incubation in fresh liquid paraffin wax at 56 °C. Paraffin blocks were cut in 10-μm thick section using a microtome. For deparaffinization and rehydration, the sections were treated three times with xylene for 5 min and then consecutively with 100, 90, and 70% ethanol for 5 min at room temperature. The sections were washed in

water, in a 1:2 mixture of water and PBS and finally in PBS for 10 min at room temperature.

For antigen retrieval, the sections were boiled in 0.1 M sodium citrate pH 6.0 in a microwave oven and cooled down to room temperature for 20 min. The sections were washed two times in PBS and incubated in methanol for 15 min and washed again with PBS at room temperature for 5 min. The sections were then incubated in blocking solution (PBS containing 1% Triton X-100 and 5% non-immune donkey serum) at room temperature for 1 h and then with primary antibodies (diluted 1:100 in blocking solution) in a humidified chamber at 4 °C overnight. The sections were washed three times with PBS and incubated with fluorescently labeled secondary antibodies (diluted 1:200 in blocking solution) in the dark at room temperature for 1 h. Sections were washed three times with PBS for 10 min and stained with DAPI solution (Sigma-Aldrich) for 10 min. The sections were washed in PBS and mounted in Dako Fluorescent Mounting Medium S3023 (Dako, Glostrup, Denmark).

For Golgi silver impregnation and Nissl staining, freshly fixed brains were cut sagittally and immersed twice in deionized water. Following incubation in 2% aqueous potassium dichromate solution at room temperature under gentle agitation for 11 h in the dark, brains were washed twice in deionized water, rinsed twice in 2% aqueous silver nitrate solution, and incubated in this solution for further 11 h in the dark. After washing in deionized water twice, sagittal vibratome sections of 70-μm thickness were cut in deionized water. Sections were air dried, and counterstained with cresyl violet.

Images were taken on a confocal fluorescence microscope (Olympus, Hamburg, Germany) or a Keyence Fluorescent Microscope (BZ-9000, Keyence, Neu-Isenburg, Germany), and quantifications were performed with the Hybrid cell count software (Keyence) and the ImageJ software. For the assessment of synaptic coverage, the number of GAD67- and vGlut1-immunopositive puncta per area were determined in each cerebellar layer. For the identification of the cerebellar layers, the apical and distal soma edges of the Purkinje cells were used as reference points for setting the borders to the molecular layer and granule cell layer.

Images of Golgi impregnated Purkinje cells were processed with the ImageJ software for Sholl analysis according to instructions of the software macro (Sholl analysis macro, Fiji, https://imagej.net/Fiji) to assess the number of intersections in each 5-μm sector out of 50 sectors that had been projected radially from the soma of each impregnated Purkinje cell following the main dendritic branches. Polynomial interpolation of the sixth degree was then applied using the GraphPrism software (GraphPad, La Jolla, CA, USA) to assess the maximal radius corresponding to the highest intersection number. The number and area of dendritic spines on primary branches (first branches from the main dendritic branch) were assessed with the ImageJ software and were referred to the area of the corresponding primary branches.

Electron microscopy on Epon-embedded cerebellar neurons and tissue was performed as described [43].

ELISA

Recombinant proteins were diluted to 5 μg/ml in PBS, and 25 μl of the dilutions per well were used for coating at 4 °C overnight in 384-well microtiter plates with high binding surface (Corning, Tewksbury, MA, USA). After washing with PBS for 30 s, the wells were incubated with 2% essentially fatty acid-free BSA (Sigma-Aldrich) in PBS at room temperature for 1 h, washed with PBS for 30 s, and incubated with nuclear extracts from transduced cerebellar neurons (12 μg of nuclear proteins per well) at room temperature for 1 h. After washing three times with PBS for 30 s, rabbit L1 antibody (diluted 1:100 in PBS) was applied for 1 h. The ELISA plate was washed three times for 5 min with PBS with 0.05% Tween (PBST) and incubated for 1 h with horseradish peroxidase secondary antibody (diluted 1:2000 in PBS). The plate was rinsed again two times with PBS for 30 s and three times for 5 min with PBST. The reaction was developed with orthophenylenediamine dihydrochloride (ThermoFisher Scientific), which was added at a concentration of 1 mg/ml and incubated for 0.5–5 min. The color reaction was terminated with 2.4 M sulfuric acid and the absorption was measured at 492 nm using the μQuantTM microplate spectrophotometer (Bio-Tek Instruments, Bad Friedrichshall, Germany).

Biometrics, Muscle Strength Assessment, Rotarod, and Pole Tests

The sample size (number of mice) required for a reliable statistic conclusion needed for the rotarod and pole tests was iteratively estimated using the G*Power Software (Düsseldorf) and assuming a priori a type I error $\alpha = 0.05$ and aiming at a Cohen effect $d \geq 0.2$ [44]. We have used published data on locomotor behavior [45–49] as a reference to estimate the variation of means among the genotype groups. The estimated values of variation were then iteratively transferred to the behavioral tests of the present study for optimization of the sample size.

To evaluate muscle strength, mice were held by the tail and the strength of the forelimbs was measured with a Grip Strength Meter system (TSE Systems, Bad Homburg, Germany).

An accelerating rotarod for mice (Ugo Basile S.R.L., Comerio, Italy) was used to analyze motor coordination. The rod was started to rotate 5 s after the mice were placed onto it. Mice underwent three training sessions and five test sessions. The training sessions were performed on the first day with a constant rotating speed of 4 rpm for a maximal duration of

1 min and an inter-trial interval of 10 min. The test trials were performed on 5 consecutive days every morning and afternoon with accelerating speeds from 4 rpm up to 40 rpm within 300 s. The durations until falling off the rod (latency to fall) and the rotation speeds at which the mice fell down were recorded.

For the pole test, mice were placed head upward on top of a vertical 48.5-cm long pole made of rough wood with a diameter of 0.8 cm. The time needed to climb down the vertical pole was measured on 5 consecutive days in three test trial each day with a maximum duration of 40 s and an inter-trial interval of 30 s.

qPCR

RNA was isolated from brains using TRI Reagent® (Sigma-Aldrich, Taufkirchen, Germany), followed by further RNA purification using the RNeasy Plus Kit (Qiagen, Hilden, Germany). For reverse transcription, oligoT_{18} primer and reverse transcriptase (Sigma-Aldrich) were used. qPCR was performed in triplicates using reverse transcribed mRNA, the 7900HT Fast Real-Time PCR System (ThermoFisher Scientific), the qPCR kit SYBR® Green I, ROX (Eurogentec, Cologne, Germany), and primers for determination of mRNA levels of PSCK9 and LDLR. The primers are PCSK9 fw(5'-ACG TGG CCG GCA TTG TG-3'), PCSK9 rev (5'-GAG AAG TGG ATC AGC CTC TGC CGC AG-3'), LDLR fw (5'-AAG GCT GTC CCC CCA AGA-3' or 5'-GGC ATC ACA CTA GGA CAA AGT-3'), and LDLR rev (5'-GAT GAG TTG CAG CGG AAG T-3' or 5'-GGG CTG TTG TCT CAC ACC AGT T-3'). The SDS 2.4 software (ThermoFisher Scientific) was used for analysis of the qPCR data, and the mRNA levels relative to the mRNA levels of the reference genes GAPDH, tubulin, and actin were calculated.

Results

L1-70 Interacts with Distinct Nuclear Receptors Via the LXXLL and FXXLF Motifs

By bioinformatic analysis, we found that L1 harbors two motifs, LXXLL (L_{1136}LILL) and FXXLF (F_{1046}HILF), which are present also in co-activators and co-repressors that bind to nuclear receptors (for reviews and references, see [30–37]). Since these motifs are present in L1-70 which enters the nucleus [25], we asked whether nuclear L1-70 associates with the nuclear receptors AR, ERα, RXR, and PPARγ. To address this question, we performed immunoprecipitation using a nuclear extract from mouse brains and the L1 antibody 555 which recognizes an epitope in the extracellular L1 domain and subjected the L1 immunoprecipitates to immunoblot analysis with antibodies against the nuclear receptors AR, ERα, RXR, and PPARγ. L1 immunoprecipitates contained ERβ, RXR, PPARγ, but not AR (Fig. 1a). Non-immune control IgG did not co-immunoprecipitate these receptors (Fig.1a). The results suggested that nuclear L1-70 can associate with distinct nuclear receptors, such as ERβ, RXR, and PPARγ.

We then investigated whether the association of nuclear L1-70 with ERβ, RXR, and PPARγ is mediated by the LXXLL and FXXLF motifs of L1-70. We first tested whether mutations of these motifs would affect the generation and nuclear import of L1-70. Hence, cultured L1-deficient cerebellar neurons were transduced with AAV1 coding for wild-type L1 or for L1 with mutated nuclear receptor motifs (exchange of L_{1136}LILL to A_{1136}LIAA and F_{1046}HILF to Y_{1046}HIAY). We subjected the nuclear fractions from the transduced neurons to immunoblot analysis with L1 antibody 172 which recognizes an epitope in the intracellular L1 domain. L1-70 was detected in the nuclear fractions from L1-deficient neurons after transduction with AAV1 coding for wild-type and mutated L1 as well as in the nuclear fractions from control wild-type neurons, when compared to nuclear fractions and cell lysates from L1-deficient neurons which served as negative controls (Fig. 1b). This result indicates that the mutated nuclear receptor motifs of L1 do not affect the generation and nuclear import of L1-70. Of note, the nuclear levels of wild-type and mutated L1-70 were lower than those in wild-type neurons, suggesting that generation and nuclear import of L1-70 are more efficient in wild-type neurons than in L1-deficient neurons expressing L1 after transduction with L1-coding AAV.

We then applied the nuclear fractions from the transduced neurons containing the L1-70 in ELISA as ligands to substrate-coated recombinant AR, ERα, ERβ, PPARγ, LXRβ, VDR, and RXRβ. Nuclear fractions from neurons transduced with AAV1 encoding wild-type L1 showed a pronounced binding of nuclear L1-70 to recombinant RXRβ, PPARγ, ERα, and ERβ, but not to AR, VDR and LXRβ, relative to nuclear fractions from neurons transduced with empty AAV1 or with AAV1 coding for the mutant L1 (Fig. 2). These results indicate that L1-70 binds to RXRβ, PPARγ, ERα, and ERβ and that this binding is mediated by the motifs LXXLL and FXXLF.

It is noteworthy in this context to mention that in an unpublished study on the L1's role in lipid metabolism, we observed a dysregulated gene expression of proprotein convertase subtilisin/kexin type 9 (PCSK9) and low-density lipoprotein receptor (LDLR) in brains of 8- to 12-week-old L1-deficient mice relative to wild-type mice. Compared with mRNA levels in wild-type brains, the PCSK9 and LDLR mRNA levels were increased (2.232 ± 0.279 and 1.609 ± 0.098; $n = 4$; $p < 0.05$, Kruskal-Wallis test with post hoc Dunn's multiple comparison) in L1-deficient brains. Interestingly, the expression levels of PCSK9 and LDLR, which are key players in cholesterol metabolism (for reviews

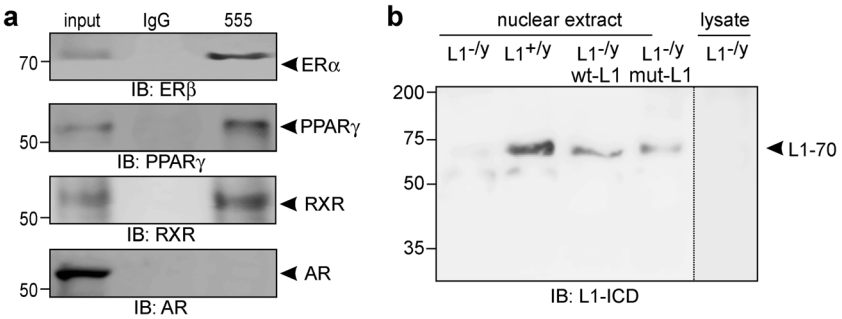

Fig. 1 Nuclear L1 co-immunoprecipitates with nuclear receptors. **a** Soluble nuclear proteins from mouse brain were subjected to immunoprecipitation with rat L1 antibody 555 or non-immune rat control antibody. The immunoprecipitates were probed by Western blot analysis with antibodies against ERβ, RXR, PPARγ, and AR. **b** Nuclear fractions were isolated from wild-type ($L1^{+/y}$) and L1-deficient ($L1^{-/y}$) cerebellar neurons and from L1-deficient cerebellar neurons transduced with wild-type L1 (wt-L1) or L1 mutant with disrupted LXXLL and FXXLF motifs (mut-L1). The nuclear fractions were subjected to immunoblot analysis with mouse L1 antibody 172 against the intracellular domain of L1. A lysate of L1-deficient neurons was used as a negative control. **a**, **b** Representative blots are shown and display only the regions of the blots with ERβ, RXR, PPARγ, and AR bands (**a**) or all L1 forms (**b**). The experiments were repeated once with identical results

see [50, 51]), are regulated in a PPARγ-dependent manner [52]. These results suggest that the interaction of L1-70 with distinct nuclear receptors, such as PPARγ, modulates expression of their target genes.

Disruption of the LXXLL and FXXLF Motifs in L1 Is Associated with Impaired Motor Coordination

L1-deficient mice are impaired in keeping their balance on a rotating rod [45], and mutations in the intracellular L1 domain lead to impaired motor function [46]. Moreover, mice deficient in farnesoid X receptor, thyroid receptor α or β, liver X receptor α (LXRα), LXRβ, or VDR also show an altered locomotor behavior in the rotarod test [53–57]. In addition, the FXXLF motif appears to contribute to regulating motor functions as seen for the FXXLF motif in AR [58]. Based on these findings, we analyzed whether disruption of the interaction of L1 with nuclear receptors by mutating LXXLL and/or FXXLF in L1 would affect the cognate functions of the cerebellum, such as motor coordination. We injected AAV1 encoding wild-type or mutated L1 into the third brain ventricle of L1-deficient embryos at embryonic day 16 in utero and allowed the injected embryos to develop thereafter for 12 weeks. Transduced mice and non-transduced wild-type and L1-deficient littermates were analyzed in the rotarod and pole tests. Before these tests, analysis of muscle strength was performed, showing similar muscle strength in both genotypes (wild-type mice ($n = 12$): 153.11 ± 6.11 N versus L1-deficient mice ($n = 8$): 131.37 ± 14.37 N; one-way ANOVA with multiple comparison test: no significant difference). L1-deficient mice showed a lower latency in falling off the accelerating rotarod than wild-type mice (Fig. 3a). Wild-type mice performed better in subsequent trials, whereas L1-deficient mice did not show this improvement (Fig. 3a). L1-deficient mice transduced with AAV1 coding for wild-type L1 performed as well as the wild-type mice (Fig. 3a), whereas L1-deficient mice transduced with AAV1 coding for mutated L1 did not increase their performance level as compared to the level of

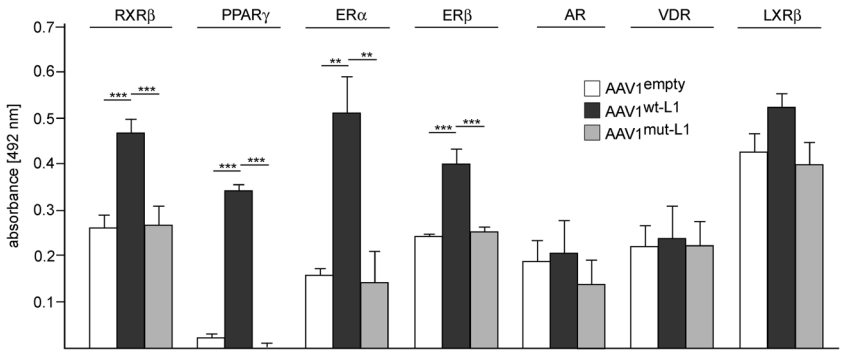

Fig. 2 Nuclear L1 interacts with nuclear receptors. Substrate-coated recombinant ERα, ERβ, RXR, PPARγ, VDR, LXRβ, and AR proteins, and nuclear fractions from L1-deficient cerebellar neurons transduced either with an empty AAV1 ($AAV1^{empty}$) or with AAV1 encoding wild-type L1 ($AAV1^{wt\text{-}L1}$) or with the L1 double mutant ($AAV1^{mut\text{-}L1}$) were taken for ELISA. Using rabbit L1CAM antibody, binding of nuclear L1 to recombinant nuclear receptors was determined. Mean values + SEM from three independent experiments with nuclear extracts from two cell culture wells on different plates per treatment for each experiment ($n = 6$) are shown for L1 binding (**$p < 0.01$, ***$p < 0.001$; one-way ANOVA with Holm-Sidak multiple comparison test)

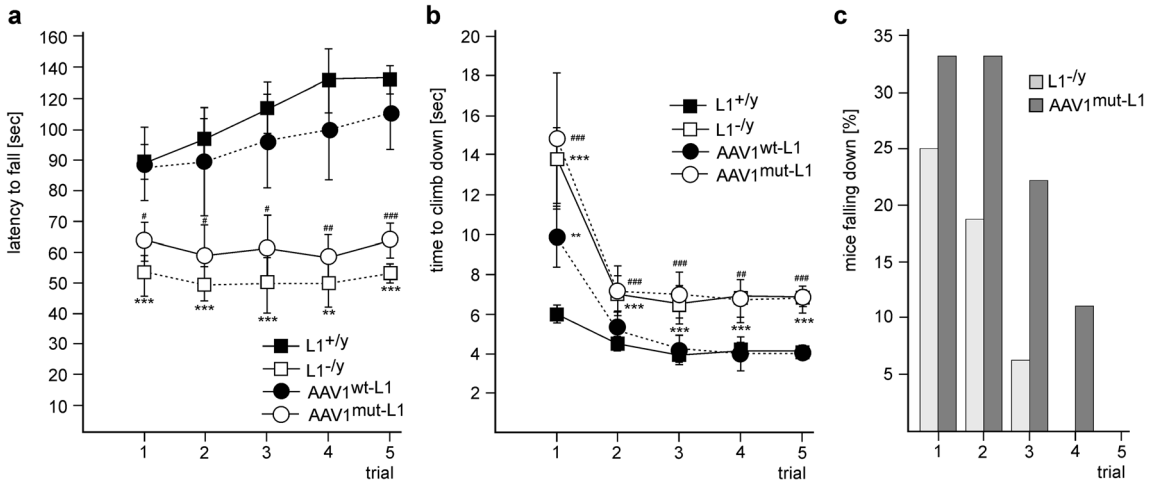

Fig. 3 Mice transduced in utero with L1 carrying disrupted LXXLL and FXXLF motifs show impaired motor coordination and learning. L1-deficient embryos were transduced with AAV1 encoding wild-type L1 or L1 with disrupted LXXLL and FXXLF motifs at embryonic day 16. Twelve weeks after transduction, the mice transduced with AAV1 encoding wild-type L1 ($AAV1^{wt\text{-}L1}$; $n = 9$) or encoding mutated L1 ($AAV1^{mut\text{-}L1}$; $n = 9$) were compared to non-transduced wild-type ($L1^{+/y}$; $n = 26$) or L1-deficient ($L1^{-/y}$; $n = 16$) mice of the same age in their ability to perform the rotarod (**a**) and pole (**b, c**) tests. The latency to fall off the rotating wheel was determined (**a**), the time needed to climb down from the top of a vertical beam was monitored (**b**), and the number of mice falling down from the top of the beam (**c**) was assessed in five trials. **a**, **b** Mean values + SEM are shown and differences relative to the wild-type group are indicated (**$p < 0.01$; ***$p < 0.001$ for L1-deficient mice, #$p < 0.05$; ##$p < 0.01$; ###$p < 0.001$ for mice transduced with AAV1 encoding mutated L1; one-way ANOVA with Holm-Sidak multiple comparison test)

the L1-deficient mice (Fig. 3a). In the pole test, L1-deficient mice needed more time to climb down from the top of a vertical beam than wild-type mice (Fig. 3b) and repeatedly fell off the top of the beam (Fig. 3c). In subsequent trials, L1-deficient mice needed less time to climb down and the percentage of mice falling down slightly decreased (Fig. 3b, c). L1-deficient mice transduced with AAV1 coding for mutated L1 performed as badly as the L1-deficient mice in the first trial (Fig. 3b, c). In subsequent trials, these mice needed more time to climb down, and the percentage of mice falling down was even higher, when compared to L1-deficient mice (Fig. 3b, c). In the first trial, L1-deficient mice transduced with AAV1 coding for wild-type L1 needed more time to climb down than the wild-type mice, but less than L1-deficient mice (Fig. 3b). In subsequent trials, L1-deficient mice transduced with AAV1 coding for wild-type L1 performed as well as the wild-type mice (Fig. 3b).

Impaired Motor Coordination in L1-Deficient Mice and Mice Expressing Mutated L1 Is Associated with Altered Synaptic Plasticity and Connectivity of Purkinje Cells

Immediately after the rotarod and pole tests were finished, the expression of L1 in the cerebellum of the mice was analyzed by immunostaining and immunoblot analysis. Immunostaining with the L1-antibody showed that wild-type and mutant L1 were expressed in cerebella of L1-deficient mice after transduction with AAV1 coding for wild-type or mutated L1, while no L1-immunopositive staining was observed in L1-deficient mice (Fig. 4a). We noticed a significant AAV1-derived expression of wild-type L1 and pronounced AAV1-derived expression of mutated L1 in Purkinje cells, while expression of L1 in these cells was hardly detectable in cerebella of wild-type mice (Fig. 4a). This observations suggest that Purkinje cells had expressed L1 only after transduction with the AAV1 coding for wild-type or mutated L1. Immunoblot analysis of brain homogenates also showed expression of L1 and L1-70 in transduced L1-deficient mice and wild-type mice, but not in non-transduced L1-deficient mice (Fig. 4b). Altogether, these results indicate that L1 and L1-70 with intact nuclear receptor motifs are required for motor coordination and motor learning.

We further investigated whether the motor control impairments after mutating the nuclear receptor motifs or complete L1-deficiency are associated with alterations in innervation of the Purkinje cells by climbing or parallel fibers, which modulate the GABAergic cerebellar output [59–61]. To this aim, we studied the ultrastructure of cerebella from the mice that had been subjected to the rotarod and pole tests. In particular, we analyzed the innervation of Purkinje cells by climbing fiber terminals and parallel fibers. In cross-section profiles, climbing fiber terminals showed a uniform distribution of synaptic vesicles in axonal terminals, which could be distinguished from other terminals that contained synaptic vesicles accumulated preferentially near postsynaptic densities. The size of the cross-section profiles of climbing fiber terminals contacting the dendritic trees of the Purkinje cells in the molecular layer was larger in wild-type mice than in L1-deficient mice. The size of terminals in wild-type mice was similar to

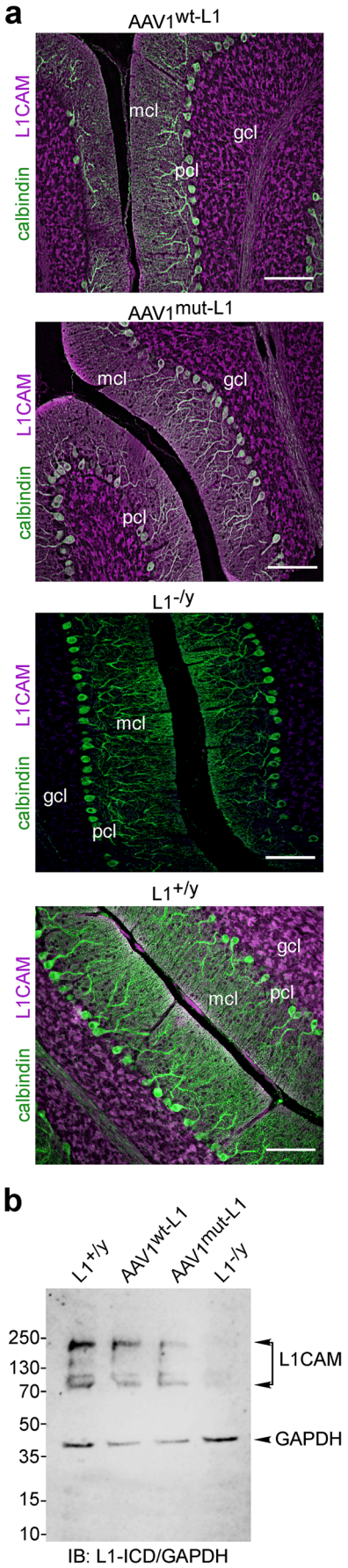

◀ **Fig. 4** L1 carrying disrupted LXXLL and FXXLF motifs is normally expressed and cleaved. After testing the mice in the rotarod and pole tests, cerebella and cerebellar homogenates obtained from wild-type ($L1^{+/y}$) and L1-deficient ($L1^{-/y}$) mice and from L1-deficient mice transduced with AAV1 encoding wild-type ($AAV1^{wt\text{-}L1}$) or mutated ($AAV1^{mut\text{-}L1}$) were subjected to immunostaining with L1 and calbindin antibodies (**a**) and to immunoblot analysis with L1CAM antibody and GAPDH antibody (**b**), respectively. **a** Representative images from two mice per group are shown. Scale bars, 200 μm. **b** A representative immunoblot is shown and displays all L1 forms, as well as the band of the loading control GAPDH. The L1 forms (L1CAM) and GAPDH band are indicated

that in mice expressing AAV-derived non-mutated L1, while the size of terminals in mice expressing the AAV-derived mutated L1 was similar to that of non-transduced L1-deficient mice (Fig. 5a, b). The density of synaptic vesicles in the climbing fiber terminals was higher in wild-type mice and in mice injected with AAV encoding non-mutated L1, when compared with the vesicle density in L1-deficient mice and in mice injected with AAV-encoding mutated L1 (Fig. 5a, b). Similarly, the cross-sectional profile area of parallel fiber terminals forming contacts with dendritic spines of Purkinje cells in the molecular layer was larger in wild-type mice and in mice expressing AAV-derived non-mutated L1 than in L1-deficient mice and in mice expressing the AAV-derived mutated L1 (Fig. 5c, d). These results indicate that the interaction of L1 with nuclear receptors is required for proper formation of synaptic contacts between climbing and parallel fiber terminals and Purkinje cells dendrites.

Next, we analyzed the arborization of the dendritic trees of Purkinje cells after Golgi staining. Purkinje cells in L1-deficient cerebella displayed less arborization of the dendritic trees and a reduced density of dendritic spines relative to Purkinje cells in wild-type cerebella (Fig. 5e–g). Purkinje cells in L1-deficient mice expressing AAV-derived wild-type L1 showed a slightly reduced branching and dendritic spine density compared with wild-type Purkinje cells (Fig. 5f, g). On the other hand, dendrites of Purkinje cells in L1-deficient mice with AAV-encoding mutant L1 showed a remarkably reduced extent of branching with decreased spine density and aberrant spine morphology, particularly in apical dendritic regions, compared with Purkinje cells from wild-type mice and L1-deficient mice expressing AAV-derived wild-type L1 (Fig. 5f, g). These results indicate that arborization of Purkinje cell dendrites and adequate formation of dendritic spines depends on the interaction of L1 with nuclear receptors.

Since stellate cells, basket cells, and granule cells play a key role in modulating the synaptic activity of Purkinje cells, we examined whether the innervation of Purkinje cells by parallel fibers of glutamatergic granule cells and by GABAergic basket and stellate cells was altered in L1-deficient mice and in mice with AAV-encoding mutant L1 relative to wild-type mice and mice with AAV-encoding wild-type L1. Based on these findings, we visualized the

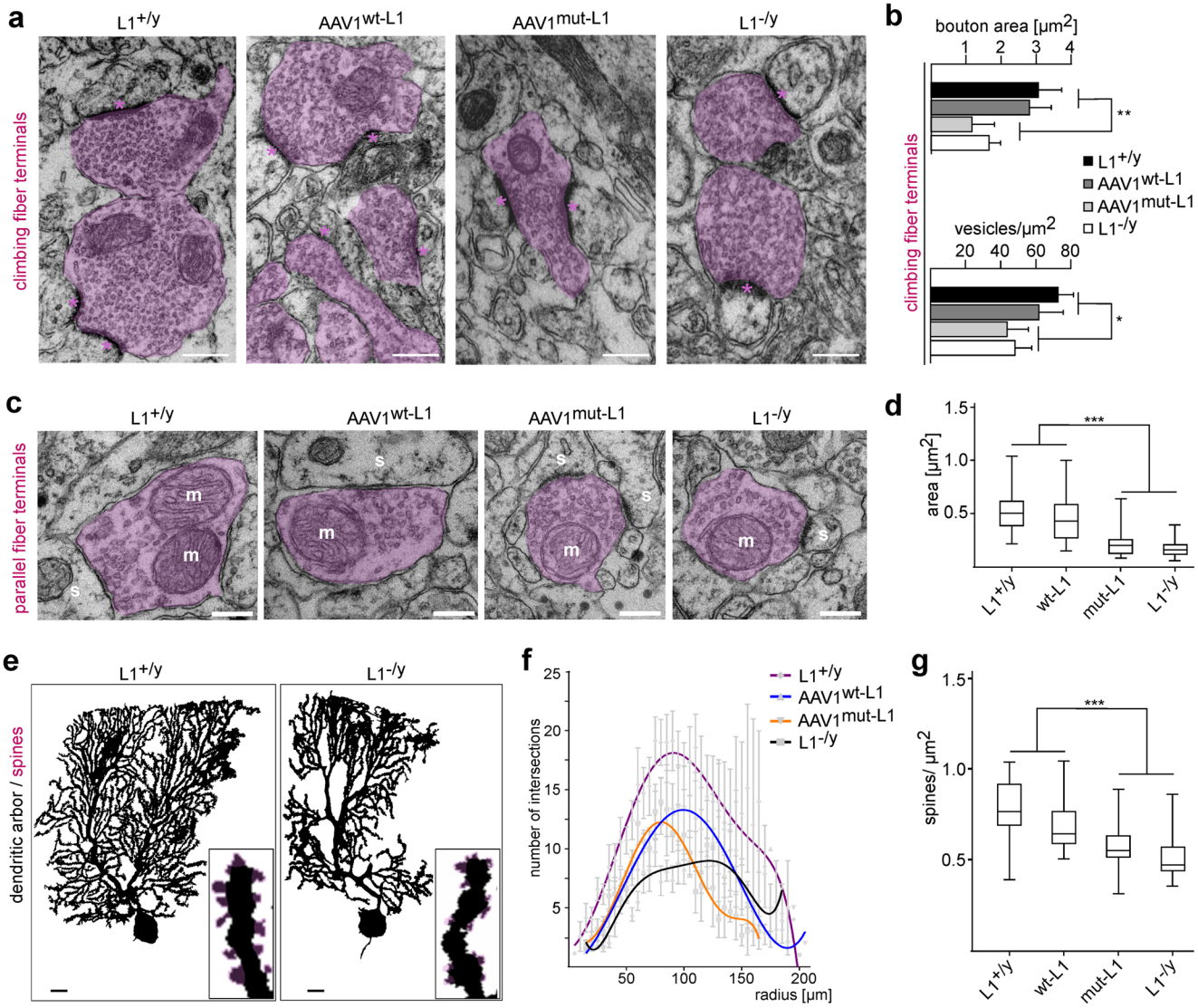

Fig. 5 Mice expressing L1 with disrupted LXXLL and FXXLF motifs show impaired innervation of Purkinje cells by climbing and parallel fiber terminals and altered morphology of Purkinje cell dendrites. After testing the mice in the rotarod and pole test, the ultrastructure of cerebellar specimens from wild-type ($L1^{+/y}$) and L1-deficient ($L1^{-/y}$) mice and from L1-deficient mice transduced with AAV1 encoding wild-type ($AAV1^{wt\text{-}L1}$) or mutated ($AAV1^{mut\text{-}L1}$) L1 was analyzed by electron microscopy. **a** Climbing fiber terminals with a characteristic homogenous distribution of vesicles are highlighted in pink. Scale bars, 250 nm. **b** Number of boutons and vesicles per area were quantified. Mean values + SD from 50 bouton profiles in randomized ultrathin sections from two mice per group are shown (one-way ANOVA with multiple comparison test; $*p < 0.05$; $**p < 0.01$). **c** Parallel fiber terminals contacting dendritic spine(s) are highlighted in pink; m mitochondria; scale bars, 250 nm. **d** Numbers of parallel fiber boutons per area were quantified. Box plots from 47 bouton profiles in randomized ultrathin sections from two mice per group are shown (one-way ANOVA with multiple comparison test; $***p < 0.001$). **e** Representative Golgi-stained Purkinje cells from wild-type ($L1^{+/y}$) and L1-deficient ($L1^{-/y}$) mice are shown. Scale bars, 10 µm; insets show dendritic branches with spines (highlighted in pink) at higher magnification. **f** Numbers of intersections at different distances from the cell bodies were determined using Sholl analysis of values obtained from randomly imaged impregnated Purkinje cells from three mice per group (for $L1^{+/y}$, $AAV1^{wt\text{-}L1}$, $AAV1^{mut\text{-}L1}$, and $L1^{-/y}$ $n = 25$, 35, 47, and 38 Purkinje cells, respectively). Polynomial interpolation of the 6th degree was applied to estimate the maximal radius (R_{max}) corresponding to the highest intersection number (X_{max}) on totally analyzed values for $L1^{+/y}$, $AAV1^{wt\text{-}L1}$, $AAV1^{mut\text{-}L1}$, and $L1^{-/y}$ of $n = 150$, 194, 322, and 218, respectively ($L1^{+/y}$: $R_{max} = 82.55$ µm, $X_{max} = 17.85$; $AAV1^{wt\text{-}L1}$: $R_{max} = 88.12$ µm, $X_{max} = 12.94$; $AAV1^{mut\text{-}L1}$: $R_{max} = 76.97$ µm, $X_{max} = 12.21$; $L1^{-/y}$: $R_{max} = 84.10$ µm, $X_{max} = 8.29$). **g** Box plots are shown for the numbers of dendritic spines per primary branch area in the impregnated Purkinje cells used for the Sholl analysis (for $L1^{+/y}$, $AAV1^{wt\text{-}L1}$, $AAV1^{mut\text{-}L1}$, and $L1^{-/y}$ $n = 25$, 35, 47, and 38 spines, respectively; one-way ANOVA with multiple comparison test; $***p < 0.001$)

synaptic contacts and synaptic cell coverage in cerebellar sections by immunostaining for the GABAergic cell marker GAD67 and the glutamatergic cell marker vGlut1 and assessed the number of immunopositive puncta. In the cerebella of wild-type mice and of mice expressing AAV-derived wild-type L1, higher numbers of GAD67-positive puncta were seen on Purkinje cell dendrites in the molecular layer, perisomatically and at the initial

segment of the Purkinje cells, whereas in L1-deficient mice and in mice expressing AAV-derived mutant L1, only a few puncta were seen on Purkinje cell dendrites and somata, and at the axon initial segment areas of Purkinje cells (Fig. 6a, b). Similarly, cerebella of wild-type mice and of mice with AAV-encoding wild-type L1 showed higher numbers of vGlut1-positive puncta in the molecular layer, Purkinje cell layer, and inner granule cell layer than cerebella of L1-deficient mice and in mice with AAV-encoding L1 mutant (Fig. 6c, d). These results indicate that the interaction of L1 with nuclear receptors is required for the efficient innervation of Purkinje cells by synaptic terminals of granule, stellate, and basket cells.

Discussion

Identification and characterization of numerous intra- and extracellular interaction partners for L1 have extended the knowledge on the molecular mechanisms underlying neural L1 functions and shed light on the multiple functions of cell adhesion molecules in general (for reviews, see [1–8]). In the present study, we searched for motifs in L1 by bioinformatics with the aim to identify binding domains for novel L1 interaction partners and identified a LXXLL motif in the transmembrane domain and a FXXLF motif in the extracellular domain in the fifth fibronectin type III repeat of L1. The motifs mediate interactions to nuclear receptors and are present in all known mammalian L1 sequences, but not in sequences coding for other functionally and structurally related neural cell adhesion molecules of the immunoglobulin superfamily, such as NCAM and CHL1. This finding suggests that the nuclear receptors specifically bind to the transmembrane and extracellular L1 domains via the LXXLL and FXXLF motifs.

Nuclear receptor proteins contain a centrally located DNA-binding domain and a C-terminal ligand binding domain, which also contains the transcriptional activation function 2 (for review, see [32]). The transcriptional activation function 2 mediates the recruitment of LXXLL motif-carrying co-activators and co-repressors which interact with chromatin-remodeling proteins to promote or inhibit transcription (for review and references, see [30–32]).

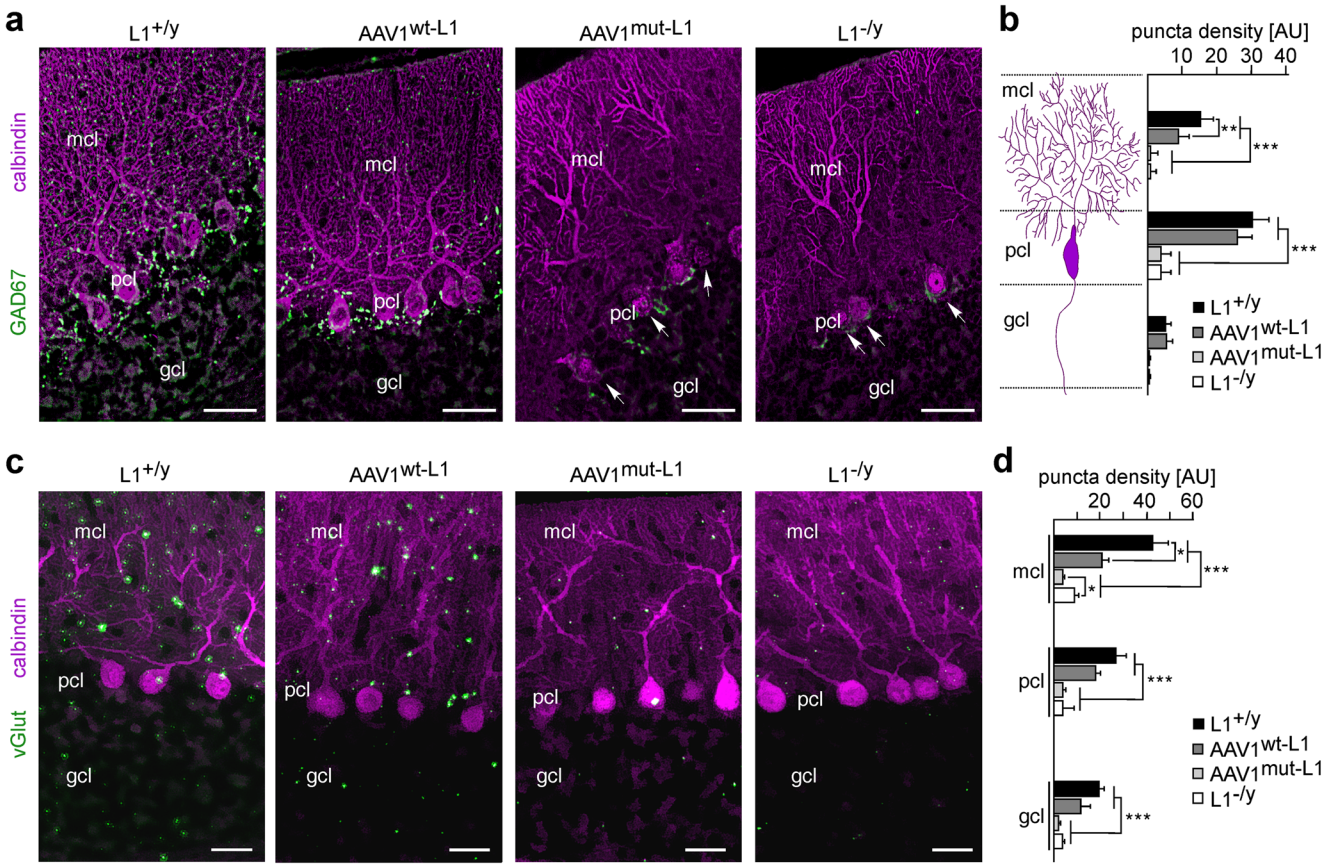

Fig. 6 Innervation of Purkinje cells by GABAergic and glutamatergic terminals is impaired in mice expressing L1 with disrupted LXXLL and FXXLF motifs. After testing the mice in the rotarod and pole tests, cerebellar specimens from wild-type ($L1^{+/y}$) and L1-deficient ($L1^{-/y}$) mice and from L1-deficient mice transduced with AAV1 encoding wild-type ($AAV1^{wt\text{-}L1}$) or mutated ($AAV1^{mut\text{-}L1}$) were analyzed by immunostaining for calbindin and GAD67 (**a**) or vGlut1 (**c**). Density of GAD67-positive (**b**) and vGlut-1-positive (**d**) puncta in the molecular layer (mcl), Purkinje cell layer (pcl), and internal granule cell layer (gcl) were quantified. Scale bars, 50 μm. Mean values + SEM from four images of sections from two mice per group are shown (*$p < 0.05$, **$p < 0.01$, ***$p < 0.001$; two-tailed Student's t test)

Binding of cognate ligands induces a conformational change in the ligand binding domain and modulates the interaction of nuclear receptors with co-activators or co-repressors. The FXXLF motif has been found in the androgen receptor (AR) and AR-specific co-activators [35–37]. Upon ligand binding, the FXXLF motif in the N-terminal domain of AR interacts with the transcriptional activation function 2 in the C-terminal ligand-binding domain of AR, and this intramolecular interaction stabilizes the ligand-receptor complex [33–37]. It is conceivable that also intermolecular interactions between the FXXLF motifs in co-activators or co-repressors and the transcriptional activation function 2 in nuclear receptors stabilize ligand-bound nuclear receptors and/or enhance or block the interaction of LXXLL motif-containing co-activators and co-repressors. Thus, the presence of the LXXLL and FXXLF motifs in L1-70 suggests that nuclear L1-70 functions as a co-activator or co-repressor of nuclear receptors and participates in promotion or inhibition of transcription regulated by nuclear receptors and their ligands. In an unpublished study, we observed that the absence of L1-70 in brains of L1-deficient mice leads to alterations in the expression of the PPARγ target genes PCSK9 and LDLR. Thus, we suggest that L1-70 is involved in regulation of transcription by nuclear receptors. Since the nuclear receptors regulate the expression of many target genes, it will be very difficult to analyze in detail which target genes of which nuclear receptor are regulated in a L1-70-dependent manner, and therefore, such analyses would be beyond the scope of the present study.

Ablation of L1 or disruption of LXXLL and FXXLF motifs is associated with impairments in motor coordination and learning. Accuracy and learning of coordinated movements are controlled by the cerebellum and depend on the modulation of the cerebellar output at the level of Purkinje cells [60, 61], which modulate the activity of neurons in the deep cerebellar nuclei. The activity of Purkinje cells is affected by excitatory inputs from climbing fibers and parallel fibers and by inhibitory inputs from basket and stellate cells. Basket cells send their projections onto the soma and the axon initial segment area of Purkinje cells, while stellate and granule cells innervate Purkinje cell dendrites. Climbing fiber terminals are present on dendrites, cell bodies, and axon initial segment area of Purkinje cells. We show that the lack of L1 or mutation of the LXXLL and FXXLF motifs resulted in structural alterations in the cerebellum. The ultrastructural formation of climbing fiber and parallel fiber terminals on Purkinje cell dendrites was impaired, arborization of Purkinje cell dendrites was abnormal, and the density of dendritic spines on Purkinje cells dendrites was reduced. Since the Purkinje cells receive multiple synaptic inputs from granules, stellate, and basket cells, an abnormal dendritic arborization would imply abnormal formation of synaptic contacts with these cells, suggesting a regulatory role of the interplay between L1 and nuclear receptors in synaptic contact formation. An expression of L1 protein has been detected only in granule cells, but not in stellate or basket cells, and not on dendrites or cell bodies of Purkinje cells [62]. Here, we did not observe significant expression of L1 in Purkinje cells of cerebella from wild-type mice indeed. In contrast, several Purkinje cells expressed L1 after transduction with AAV1 coding for wild-type or mutated L1. Thus, it seemed conceivable that the interaction of nuclear L1 with nuclear receptors in wild-type granule cells triggers events which have an impact on stellate, basket, and Purkinje cells to regulate the formation of synaptic contacts between these cells. Disturbance of the interaction of nuclear L1 with nuclear receptors or absence of L1 in granule cells may perturb formation of connections between Purkinje cells and stellate cell and/or basket cell projections. The changes in this cerebellar circuitry under L1 deficiency or upon disruption of the L1-motifs LXXLL and FXXLF may therefore lead to motor dyscoordination and impaired learning.

By ELISA, we showed that nuclear L1 binds to ERα, ERβ, RXRβ, and PPARγ, but not to LXRβ, AR, and VDR. Based on these results, we propose that the nuclear L1 fragment L1-70 interacts with distinct nuclear receptors and that the interaction of L1-70 with nuclear receptors not only depends on the LXXLL and FXXLF motifs in L1 but also on certain conformations of nuclear receptors and/or binding of a distinct ligand to nuclear receptors or on other L1 sequences or other unknown factors.

ERβ mRNA and protein are expressed in granule, basket, and stellate, but not or at low levels in Purkinje cells [63–68]. ERα mRNA has been found in granule cells, while ERα protein was predominantly found in Purkinje cells [69]. ERα and ERβ mediate many of the effects of estradiol, which is an important regulator of the function and plasticity of the adult central nervous system, and they affect important developmental processes such as proliferation, migration, synapse formation, and apoptosis (for review, see [68]). Estradiol is locally synthesized in the cerebellum, directs cerebellar development, and affects cerebellar glutamatergic neurotransmission, and locomotor abilities, as well as other cerebellar functions (for reviews, see [68, 70]). In addition, estradiol plays a beneficial role in aging; improves balance, coordination, and mobility of post-menopausal women; and has been implicated in neuroprotection in neurological disorders, such as Alzheimer's disease, Friedreich's ataxia, and premenstrual dysphoric disorder (for review, see [68]). Furthermore, estradiol protects cerebellar neurons against toxic insults, e.g., caused by ethanol. Estradiol treatment of animals counteracts the effects of ethanol application and withdrawal, e.g., cerebellar neurodegeneration is reduced, and the performance in an accelerated rotarod test is improved [71].

It is noteworthy to mention that estradiol is locally synthesized in men and women not only in the cerebellum but also in other brain regions [72–75], where it contributes to the regulation of brain functions, such as memory, cognition, behavior, and mood.

Nuclear L1 interacts with PPARγ and RXRβ which are one of three PPAR and RXR isoforms besides PPARα, PPARβ, RXRα, and RXRγ, respectively. The RXRs act either as homodimers or form heterodimers with a number of nuclear receptors and are activated not only by 9-cis retinoic acid but also by the Δ-3 polyunsaturated fatty acid (PUFA) docosahexaenoic acid and the Δ-6 PUFA arachidonic acid [76, 77]. PPARs act as heterodimers with RXRs and play an important role in the regulation of lipid metabolism. PPARs are activated by fatty acids, e.g., the Δ-3 PUFA eicosapentaenoic acid [78] and by eicosanoids which are polyunsaturated lipids derived from the arachidonic acid metabolism. PPARγ and RXRβ are expressed in granule cells [79–85], while stellate and basket cells, but not Purkinje cells, are PPARγ-positive and lack RXRβ [84]. Of note, retinoic acid is essential for central nervous system development, and the lack of retinoic acid or defective retinoic acid signaling via RXRs causes neurodegeneration, being further associated with Alzheimer's disease [86, 87]. PUFAs play a central role in the development and functioning of the central nervous system and imbalances in PUFA levels are often associated with neurological and psychiatric disorders, such as attention-deficit hyperactivity disorder, bipolar disorders, and autism spectrum disorders (for review, see [88]). In addition, an implication of PUFAs in "alcohol use disorders" and fetal alcohol syndromes has been proposed [89–91]. Moreover, ethanol inhibits activation of RXRβ in granule cells in a rodent model of fetal alcohol spectrum disorders [83].

L1 has numerous functions during neural development and plays an important role in neurite outgrowth, axon pathfinding, and fasciculation. Moreover, L1 has been implicated as a target for the neurotoxic and teratogenic effects of ethanol, being associated with fetal alcohol spectrum disorders characterized by mental retardation, ataxia, hyperactivity, and epilepsy [92–95]. Ethanol affects neural cell adhesion, migration, survival, and communication as well as development of axons, dendrites, and synapses. Chronic ethanol uptake not only leads to ataxia but also causes cerebellar degeneration, characterized by atrophy of Purkinje cell dendrites, loss of Purkinje cells, and shrinkage of cerebellar white matter. Prenatal alcohol exposure induces death of Purkinje and granule cells and impairs differentiation, neurite outgrowth, synapse formation, and neuronal signaling [96]. Hence, based on the collective findings by us and others, we propose that ethanol may promote harmful effects in cerebellar granule cells by targeting RXRs, PPARs or ERs, and L1 and/or by disrupting the interaction of nuclear L1 with nuclear receptors.

Since L1 plays important roles in central and peripheral nervous system under physiological and pathological conditions, it is likely that the interaction of nuclear L1 with ERα, ERβ, RXRβ, PPARγ, or nuclear receptors, which have not been tested in this study, may contribute to the regulation of L1 functions in the intact, injured, or diseased nervous systems.

Since there is growing evidence that the cerebellum is involved in cognitive function and since L1 plays important roles in other brain regions, we do not exclude the possibility that the interaction of nuclear L1 with nuclear receptors in the cerebellum and other brain regions may be involved in the regulation of cognitive function and may contribute to the pathology of autism, attention-deficit hyperactivity disorder, schizophrenia, and depression.

In conclusion, we would like to state that L1 acts in a newly discovered mechanism as a co-activator of nuclear transcription factors, thus influencing specific cell interactions at the molecular and network levels.

Acknowledgements We are grateful to Eva Kronberg for the excellent animal care and to Ute Bork and Dagmar Drexler for the excellent technical assistance.

Funding Information D.L. is supported by a FFM fellowship of the Medical Faculty, University Medical Center Hamburg-Eppendorf. D.L. is grateful for the support by the Hertie Foundation. M.H. is supported by the Egyptian Cultural Bureau Berlin, Egyptian Ministry of Higher Education, and the Egyptian Missions Sector. M.S. is grateful for the support by the Li Kashing Foundation at Shantou University Medical College.

Compliance with Ethical Standards Experiments were carried out and the manuscript was prepared following the ARRIVE guidelines for animal research [39].

Conflict of Interest The authors declare that they have no conflict of interest.

References

1. Kamiguchi H, Hlavin ML, Lemmon V (1998) Role of L1 in neural development: what the knockouts tell us. Mol Cell Neurosci 12(1-2):48–55. https://doi.org/10.1006/mcne.1998.0702
2. Hortsch M (2000) Structural and functional evolution of the L1 family: Are four adhesion molecules better than one? Mol Cell Neurosci 15(1):1–10. https://doi.org/10.1006/mcne.1999.0809
3. Hortsch M, Nagaraj K, Mualla R (2014) The L1 family of cell adhesion molecules: a sickening number of mutations and protein functions. Adv Neurobiol 8:195–229
4. Loers G, Schachner M (2007) Recognition molecules and neural repair. J Neurochem 101(4):865–882. https://doi.org/10.1111/j.1471-4159.2006.04409.x
5. Maness PF, Schachner M (2007) Neural recognition molecules of the immunoglobulin superfamily: signaling transducers of axon guidance and neuronal migration. Nat Neurosci 10(1):19–26. https://doi.org/10.1038/nn1827
6. Schmid RS, Maness PF (2008) L1 and NCAM adhesion molecules as signaling coreceptors in neuronal migration and process outgrowth. Curr Opin Neurobiol 18(3):245–250. https://doi.org/10.1016/j.conb.2008.07.015

7. Schäfer MK, Altevogt P (2010) L1CAM malfunction in the nervous system and human carcinomas. Cell Mol Life Sci 67(14): 2425–2437. https://doi.org/10.1007/s00018-010-0339-1
8. Sytnyk V, Leshchyns'ka I, Schachner M (2017) Neural cell adhesion molecules of the immunoglobulin superfamily regulate synapse formation, maintenance, and function. Trends Neurosci 40(5): 295–308. https://doi.org/10.1016/j.tins.2017.03.003
9. Poltorak M, Khoja I, Hemperly JJ, Williams JR, El-Mallakh R, Freed WJ (1995) Disturbances in cell recognition molecules (N-CAM and L1 antigen) in the CSF of patients with schizophrenia. Exp Neurol 131(2):266–272. https://doi.org/10.1016/0014-4886(95)90048-9
10. Fransen E, Vits L, Van Camp G, Willems PJ (1996) The clinical spectrum of mutations in L1, a neuronal cell adhesion molecule. Am J Med Genet 64(1):73–77. https://doi.org/10.1002/(SICI)1096-8628(19960712)64:1<73::AID-AJMG11>3.0.CO;2-P
11. Fransen E, Lemmon V, Van Camp G, Vits L, Coucke P, Willems PJ (1995) CRASH syndrome: clinical spectrum of corpus callosum, hypoplasia, retardation, adducted thumbs, spastic paraparesis and hydrocephalus due to mutations in one single gene, L1. Eur J Hum Genet 3(5):273–284. https://doi.org/10.1159/000472311
12. Kurumaji A, Nomoto H, Okano T, Toru M (2001) An association study between polymorphism of L1CAM gene and schizophrenia in a Japanese sample. Am J Med Genet 105(1):99–104. https://doi.org/10.1002/1096-8628(20010108)105:1<99::AID-AJMG1071>3.0.CO;2-U
13. Strekalova H, Buhmann C, Kleene R, Eggers C, Saffell J, Hemperly J, Weiller C, Müller-Thomsen T et al (2006) Elevated levels of neural recognition molecule L1 in the cerebrospinal fluid of patients with Alzheimer disease and other dementia syndromes. Neurobiol Aging 27(1):1–9. https://doi.org/10.1016/j.neurobiolaging.2004.11.013
14. Wakabayashi Y, Uchida S, Funato H, Matsubara T, Watanuki T, Otsuki K, Fujimoto M, Nishida A et al (2008) State-dependent changes in the expression levels of NCAM-140 and L1 in the peripheral blood cells of bipolar disorders, but not in the major depressive disorders. Prog Neuro-Psychopharmacol Biol Psychiatry 32(5):1199–1205. https://doi.org/10.1016/j.pnpbp.2008.03.005
15. Sadoul K, Sadoul R, Faissner A, Schachner M (1988) Biochemical characterization of different molecular forms of the neural cell adhesion molecule L1. J Neurochem 50(2):510–521. https://doi.org/10.1111/j.1471-4159.1988.tb02941.x
16. Silletti S, Mei F, Sheppard D, Montgomery AM (2000) Plasmin-sensitive dibasic sequences in the third fibronectin-like domain of L1-cell adhesion molecule (CAM) facilitate homomultimerization and concomitant integrin recruitment. J Cell Biol 149(7):1485–1502. https://doi.org/10.1083/jcb.149.7.1485
17. Nayeem N, Silletti S, Yang X, Lemmon VP, Reisfeld RA, Stallcup WB, Montgomery AM (1999) A potential role for the plasmin(ogen) system in the posttranslational cleavage of the neural cell adhesion molecule L1. J Cell Sci 112:4739–4749
18. Mechtersheimer S, Gutwein P, Agmon-Levin N, Stoeck A, Oleszewski M, Riedle S, Postina R, Fahrenholz F et al (2001) Ectodomain shedding of L1 adhesion molecule promotes cell migration by autocrine binding to integrins. J Cell Biol 155(4):661–673. https://doi.org/10.1083/jcb.200101099
19. Maretzky T, Schulte M, Ludwig A, Rose-John S, Blobel C, Hartmann D, Altevogt P, Saftig P et al (2005) L1 is sequentially processed by two differently activated metalloproteases and presenilin/gamma-secretase and regulates neural cell adhesion, cell migration, and neurite outgrowth. Mol Cell Biol 25(20):9040–9053. https://doi.org/10.1128/MCB.25.20.9040-9053.2005
20. Matsumoto-Miyai K, Ninomiya A, Yamasaki H, Tamura H, Nakamura Y, Shiosaka S (2003) NMDA-dependent proteolysis of presynaptic adhesion molecule L1 in the hippocampus by neuropsin. J Neurosci 23(21):7727–7736
21. Kalus I, Schnegelsberg B, Seidah NG, Kleene R, Schachner M (2003) The proprotein convertase PC5A and a metalloprotease are involved in the proteolytic processing of the neural adhesion molecule L1. J Biol Chem 278(12):10381–10388. https://doi.org/10.1074/jbc.M208351200
22. Gutwein P, Mechtersheimer S, Riedle S, Stoeck A, Gast D, Joumaa S, Zentgraf H, Fogel M et al (2003) ADAM10-mediated cleavage of L1 adhesion molecule at the cell surface and in released membrane vesicles. FASEB J 17(2):292–294. https://doi.org/10.1096/fj.02-0430fje
23. Gutwein P, Stoeck A, Riedle S, Gast D, Runz S, Condon TP, Marmé A, Phong MC et al (2005) Cleavage of L1 in exosomes and apoptotic membrane vesicles released from ovarian carcinoma cells. Clin Cancer Res 11(7):2492–2501. https://doi.org/10.1158/1078-0432.CCR-04-1688
24. Riedle S, Kiefel H, Gast D, Bondong S, Wolterink S, Gutwein P, Altevogt P (2009) Nuclear translocation and signalling of L1-CAM in human carcinoma cells requires ADAM10 and presenilin/gamma-secretase activity. Biochem J 420(3):391–402. https://doi.org/10.1042/BJ20081625
25. Lutz D, Wolters-Eisfeld G, Joshi G, Djogo N, Jakovcevski I, Schachner M, Kleene R (2012) Generation and nuclear translocation of sumoylated transmembrane fragment of cell adhesion molecule L1. J Biol Chem 287(21):17161–17175. https://doi.org/10.1074/jbc.M112.346759
26. Lutz D, Loers G, Kleene R, Oezen I, Kataria H, Katagihallimath N, Braren I, Harauz G et al (2014) Myelin basic protein cleaves cell adhesion molecule L1 and promotes neuritogenesis and cell survival. J Biol Chem 289(19):13503–13518. https://doi.org/10.1074/jbc.M113.530238
27. Lutz D, Wolters-Eisfeld G, Schachner M, Kleene R (2014) Cathepsin E generates a sumoylated intracellular fragment of the cell adhesion molecule L1 to promote neuronal and Schwann cell migration as well as myelination. J Neurochem 128(5):713–724. https://doi.org/10.1111/jnc.12473
28. Lutz D, Kataria H, Kleene R, Loers G, Chaudhary H, Guseva D, Wu B, Jakovcevski I et al (2016) Myelin basic protein cleaves cell adhesion molecule L1 and improves regeneration after injury. Mol Neurobiol 53(5):3360–3376. https://doi.org/10.1007/s12035-015-9277-0
29. Djogo N, Jakovcevski I, Müller C, Lee HJ, Xu JC, Jakovcevski M, Kügler S, Loers G et al (2013) Adhesion molecule L1 binds to amyloid beta and reduces Alzheimer's disease pathology in mice. Neurobiol Dis 56:104–115. https://doi.org/10.1016/j.nbd.2013.04.014
30. Smirnov AN (2002) Nuclear receptors: nomenclature, ligands, mechanisms of their effects on gene expression. Biochemistry (Mosc) 67(9):957–977. https://doi.org/10.1023/A:1020545200302
31. Gronemeyer H, Gustafsson JA, Laudet V (2004) Principles for modulation of the nuclear receptor superfamily. Nat Rev Drug Discov 3(11):950–964. https://doi.org/10.1038/nrd1551
32. Bain DL, Heneghan AF, Connaghan-Jones KD, Miura MT (2007) Nuclear receptor structure: implications for function. Annu Rev Physiol 69(1):201–220. https://doi.org/10.1146/annurev.physiol.69.031905.160308
33. Askew EB, Minges JT, Hnat AT, Wilson EM (2012) Structural features discriminate androgen receptor N/C terminal and coactivator interactions. Mol Cell Endocrinol 348(2):403–410. https://doi.org/10.1016/j.mce.2011.03.026
34. Dubbink HJ, Hersmus R, Pike AC, Molier M, Brinkmann AO, Jenster G, Trapman J (2006) Androgen receptor ligand-binding domain interaction and nuclear receptor specificity of FXXLF and LXXLL motifs as determined by L/F swapping. Mol Endocrinol 20(8):1742–1755. https://doi.org/10.1210/me.2005-0348
35. He B, Bowen NT, Minges JT, Wilson EM (2001) Androgen-induced NH2- and COOH-terminal interaction inhibits p160

coactivator recruitment by activation function 2. J Biol Chem 276(45):42293–42301. https://doi.org/10.1074/jbc.M107492200
36. He B, Kemppainen JA, Wilson EM (2000) FXXLF and WXXLF sequences mediate the NH2-terminal interaction with the ligand binding domain of the androgen receptor. J Biol Chem 275(30): 22986–22994. https://doi.org/10.1074/jbc.M002807200
37. He B, Minges JT, Lee LW, Wilson EM (2002) The FXXLF motif mediates androgen receptor-specific interactions with coregulators. J Biol Chem 277(12):10226–10235. https://doi.org/10.1074/jbc.M111975200
38. Dahme M, Bartsch U, Martini R, Anliker B, Schachner M, Mantei N (1997) Disruption of the mouse L1 gene leads to malformations of the nervous system. Nat Genet 17(3):346–349. https://doi.org/10.1038/ng1197-346
39. Kilkenny C, Browne WJ, Cuthill IC, Emerson M, Altman DG (2010) Improving bioscience research reporting: the ARRIVE guidelines for reporting animal research. PLoS Biol 8(6): e1000412. https://doi.org/10.1371/journal.pbio.1000412
40. Appel F, Holm J, Conscience JF, Von BohlenundHalbach F, Faissner A, James P, Schachner M (1995) Identification of the border between fibronectin type III homologous repeats 2 and 3 of the neural cell adhesion molecule L1 as a neurite outgrowth promoting and signal transducing domain. J Neurobiol 28(3): 297–312. https://doi.org/10.1002/neu.480280304
41. Xiao MF, Xu JC, Tereshchenko Y, Novak D, Schachner M, Kleene R (2009) Neural cell adhesion molecule modulates dopaminergic signaling and behavior by regulating dopamine D2 receptor internalization. J Neurosci 29(47):14752–14763. https://doi.org/10.1523/JNEUROSCI.4860-09.2009
42. Makhina T, Loers G, Schulze C, Ueberle B, Schachner M, Kleene R (2009) Extracellular GAPDH binds to L1 and enhances neurite outgrowth. Mol Cell Neurosci 41(2):206–218. https://doi.org/10.1016/j.mcn.2009.02.010
43. Westphal N, Kleene R, Lutz D, Theis T, Schachner M (2016) Polysialic acid enters the cell nucleus attached to a fragment of the neural cell adhesion molecule NCAM to regulate the circadian rhythm in mouse brain. Mol Cell Neurosci 74:114–127. https://doi.org/10.1016/j.mcn.2016.05.003
44. Cohen J (1988) Statistical power analysis for the behavioral sciences, 2nd edn. Lawrence Erlbaum Associates, Hillsdale
45. Fransen E, D'Hooge R, Van Camp G, Verhoye M, Sijbers J, Reyniers E, Soriano P, Kamiguchi H et al (1998) L1 knockout mice show dilated ventricles, vermis hypoplasia and impaired exploration patterns. Hum Mol Genet 7(6):999–1009. https://doi.org/10.1093/hmg/7.6.999
46. Nakamura Y, Lee S, Haddox CL, Weaver EJ, Lemmon VP (2010) Role of the cytoplasmic domain of the L1 cell adhesion molecule in brain development. J Comp Neurol 518(7):1113–1132. https://doi.org/10.1002/cne.22267
47. Freitag S, Schachner M, Morellini F (2003) Behavioral alterations in mice deficient for the extracellular matrix glycoprotein tenascin-R. Behav Brain Res 145(1-2):189–207. https://doi.org/10.1016/S0166-4328(03)00109-8
48. Pratte M, Rougon G, Schachner M, Jamon M (2003) Mice deficient for the close homologue of the neural adhesion cell L1 (CHL1) display alterations in emotional reactivity and motor coordination. Behav Brain Res 147(1-2):31–39. https://doi.org/10.1016/S0166-4328(03)00114-1
49. Morellini F, Schachner M (2006) Enhanced novelty-induced activity, reduced anxiety, delayed resynchronization to daylight reversal and weaker muscle strength in tenascin-C-deficient mice. Eur J Neurosci 23(5):1255–1268. https://doi.org/10.1111/j.1460-9568.2006.04657.x
50. Jeon H, Blacklow SC (2005) Structure and physiologic function of the low-density lipoprotein receptor. Annu Rev Biochem 74(1): 535–562. https://doi.org/10.1146/annurev.biochem.74.082803.133354
51. Lopez D (2008) PCSK9: an enigmatic protease. Biochim Biophys Acta 1781(4):184–191. https://doi.org/10.1016/j.bbalip.2008.01.003
52. Duan Y, Chen Y, Hu W, Li X, Yang X, Zhou X, Yin Z, Kong D et al (2012) Peroxisome proliferator-activated receptor γ activation by ligands and dephosphorylation induces proprotein convertase subtilisin kexin type 9 and low density lipoprotein receptor expression. J Biol Chem 287(28):23667–23677. https://doi.org/10.1074/jbc.M112.350181
53. Hashimoto K, Curty FH, Borges PP, Lee CE, Abel ED, Elmquist JK, Cohen RN, Wondisford FE (2001) An unliganded thyroid hormone receptor causes severe neurological dysfunction. Proc Natl Acad Sci U S A 98(7):3998–4003. https://doi.org/10.1073/pnas.051454698
54. Huang F, Wang T, Lan Y, Yang L, Pan W, Zhu Y, Lv B, Wei Y et al (2015) Deletion of mouse FXR gene disturbs multiple neurotransmitter systems and alters neurobehavior. Front Behav Neurosci 9:70
55. Huang C, Wang J, Hu W, Wang C, Lu X, Tong L, Wu F, Zhang W (2016) Identification of functional farnesoid X receptors in brain neurons. FEBS Lett 590(18):3233–3242. https://doi.org/10.1002/1873-3468.12373
56. Meffre D, Shackleford G, Hichor M, Gorgievski V, Tzavara ET, Trousson A, Ghoumari AM, Deboux C et al (2015) Liver X receptors alpha and beta promote myelination and remyelination in the cerebellum. Proc Natl Acad Sci U S A 112(24):7587–7592. https://doi.org/10.1073/pnas.1424951112
57. Sakai S, Suzuki M, Tashiro Y, Tanaka K, Takeda S, Aizawa K, Hirata M, Yogo K et al (2015) Vitamin D receptor signaling enhances locomotive ability in mice. J Bone Miner Res 30(1):128–136. https://doi.org/10.1002/jbmr.2317
58. Zboray L, Pluciennik A, Curtis D, Liu Y, Berman-Booty LD, Orr C, Kesler CT, Berger T et al (2015) Preventing the androgen receptor N/C interaction delays disease onset in a mouse model of SBMA. Cell Rep 13(10):2312–2323. https://doi.org/10.1016/j.celrep.2015.11.019
59. Kitazawa S, Wolpert DM (2005) Rhythmicity, randomness and synchrony in climbing fiber signals. Trends Neurosci 28(11):611–619. https://doi.org/10.1016/j.tins.2005.09.004
60. Takayama C (2005) Formation of GABAergic synapses in the cerebellum. Cerebellum 4(3):171–177. https://doi.org/10.1080/14734220510008012
61. Dizon MJ, Khodakhah K (2011) The role of interneurons in shaping Purkinje cell responses in the cerebellar cortex. J Neurosci 31(29): 10463–10473. https://doi.org/10.1523/JNEUROSCI.1350-11.2011
62. Persohn E, Schachner M (1987) Immunoelectron microscopic localization of the neural cell adhesion molecules L1 and N-CAM during postnatal development of the mouse cerebellum. J Cell Biol 105(1):569–576. https://doi.org/10.1083/jcb.105.1.569
63. Belcher SM (1999) Regulated expression of estrogen receptor alpha and beta mRNA in granule cells during development of the rat cerebellum. Brain Res Dev Brain Res 115(1):57–69. https://doi.org/10.1016/S0165-3806(99)00050-4
64. Belcher SM, Ma X, Le HH (2009) Blockade of estrogen receptor signaling inhibits growth and migration of medulloblastoma. Endocrinology 150(3):1112–1121. https://doi.org/10.1210/en.2008-1363
65. Jakab RL, Wong JK, Belcher SM (2001) Estrogen receptor beta immunoreactivity in differentiating cells of the developing rat cerebellum. J Comp Neurol 430(3):396–409. https://doi.org/10.1002/1096-9861(20010212)430:3<396::AID-CNE1039>3.0.CO;2-0
66. Pérez SE, Chen EY, Mufson EJ (2003) Distribution of estrogen receptor alpha and beta immunoreactive profiles in the postnatal rat brain. Brain Res Dev Brain Res 145(1):117–139. https://doi.org/10.1016/S0165-3806(03)00223-2

67. Qin J, Suh JM, Kim BJ, Yu CT, Tanaka T, Kodama T, Tsai MJ, Tsai SY (2007) The expression pattern of nuclear receptors during cerebellar development. Dev Dyn 236(3):810–820. https://doi.org/10.1002/dvdy.21060
68. Hedges VL, Ebner TJ, Meisel RL, Mermelstein PG (2012) The cerebellum as a target for estrogen action. Front Neuroendocrinol 33(4):403–411. https://doi.org/10.1016/j.yfrne.2012.08.005
69. Ikeda Y, Nagai A (2006) Differential expression of the estrogen receptors alpha and beta during postnatal development of the rat cerebellum. Brain Res 1083(1):39–49. https://doi.org/10.1016/j.brainres.2006.02.025
70. Rauf S, Soejono SK, Partadiredja G (2015) Effects of treadmill exercise training on cerebellar estrogen and estrogen receptors, serum estrogen, and motor coordination performance of ovariectomized rats. Iran J Basic Med Sci 18(6):587–592
71. Jung ME, Yang SH, Brun-Zinkernagel AM, Simpkins JW (2002) Estradiol protects against cerebellar damage and motor deficit in ethanol-withdrawn rats. Alcohol 26(2):83–93. https://doi.org/10.1016/S0741-8329(01)00199-9
72. Gillies GE, McArthur S (2010) Estrogen actions in the brain and the basis for differential action in men and women: a case for sex-specific medicines. Pharmacol Rev 62(2):155–198. https://doi.org/10.1124/pr.109.002071
73. Azcoitia I, Yague JG, Garcia-Segura LM (2011) Estradiol synthesis within the human brain. Neuroscience 191:139–147. https://doi.org/10.1016/j.neuroscience.2011.02.012
74. Barakat R, Oakley O, Kim H, Jin J, Ko CJ (2016) Extra-gonadal sites of estrogen biosynthesis and function. BMB Rep 49(9):488–496. https://doi.org/10.5483/BMBRep.2016.49.9.141
75. Fester L, Prange-Kiel J, Jarry H, Rune GM (2011) Estrogen synthesis in the hippocampus. Cell Tissue Res 345(3):285–294. https://doi.org/10.1007/s00441-011-1221-7
76. de Urquiza AM, Liu S, Sjöberg M, Zetterström RH, Griffiths W, Sjövall J, Perlmann T (2000) Docosahexaenoic acid, a ligand for the retinoid X receptor in mouse brain. Science 290(5499):2140–2144. https://doi.org/10.1126/science.290.5499.2140
77. Lengqvist J, Mata De Urquiza A, Bergman AC, Willson TM, Sjövall J, Perlmann T, Griffiths WJ (2004) Polyunsaturated fatty acids including docosahexaenoic and arachidonic acid bind to the retinoid X receptor alpha ligand-binding domain. Mol Cell Proteomics 3(7):692–6703. https://doi.org/10.1074/mcp.M400003-MCP200
78. Chambrier C, Bastard JP, Rieusset J, Chevillotte E, Bonnefont-Rousselot D, Therond P, Hainque B, Riou JP et al (2002) Eicosapentaenoic acid induces mRNA expression of peroxisome proliferator-activated receptor gamma. Obes Res 10(6):518–525. https://doi.org/10.1038/oby.2002.70
79. Kainu T, Wikström AC, Gustafsson JÅ, Pelto-Huikko M (1994) Localization of the peroxisome proliferator-activated receptor in the brain. Neuroreport 5(18):2481–2485. https://doi.org/10.1097/00001756-199412000-00019
80. Braissant O, Foufelle F, Scotto C, Dauca M, Wahli W (1996) Differential expression of peroxisome proliferator-activated receptors PPARs: tissue distribution of PPAR-alpha, -beta, and -gamma in the adult rat. Endocrinology 137(1):354–366. https://doi.org/10.1210/endo.137.1.8536636
81. Cullingford TE, Bhakoo K, Peuchen S, Dolphin CT, Patel R, Clark JB (1998) Distribution of mRNAs encoding the peroxisome proliferator-activated receptor alpha, beta, and gamma and the retinoid X receptor alpha, beta, and gamma in rat central nervous system. J Neurochem 70(4):1366–1375
82. Heneka MT, Feinstein DL, Galea E, Gleichmann M, Wüllner U, Klockgether T (1999) Peroxisome proliferator-activated receptor gamma agonists protect cerebellar granule cells from cytokine-induced apoptotic cell death by inhibition of inducible nitric oxide synthase. J Neuroimmunol 100(1-2):156–168. https://doi.org/10.1016/S0165-5728(99)00192-7
83. Kumar A, Singh CK, DiPette DD, Singh US (2010) Ethanol impairs activation of retinoic acid receptors in cerebellar granule cells in a rodent model of fetal alcohol spectrum disorders. Alcohol Clin Exp Res 34(5):928–937. https://doi.org/10.1111/j.1530-0277.2010.01166.x
84. Moreno S, Farioli-Vecchioli S, Cerù MP (2004) Immunolocalization of peroxisome proliferator-activated receptors and retinoid X receptors in the adult rat CNS. Neuroscience 123(1):131–145. https://doi.org/10.1016/j.neuroscience.2003.08.064
85. Smith SA, May FJ, Monteith GR, Roberts-Thomson SJ (2001) Activation of the peroxisome proliferator-activated receptor-alpha enhances cell death in cultured cerebellar granule cells. J Neurosci Res 66(2):236–241. https://doi.org/10.1002/jnr.1216
86. Maden M (2000) The role of retinoic acid in embryonic and post-embryonic development. Proc Nutr Soc 59(01):65–73. https://doi.org/10.1017/S0029665100000082
87. Corcoran JP, So PL, Maden M (2004) Disruption of the retinoid signalling pathway causes a deposition of amyloid beta in the adult rat brain. Eur J Neurosci 20(4):896–902. https://doi.org/10.1111/j.1460-9568.2004.03563.x
88. Schuchardt JP, Huss M, Stauss-Grabo M, Hahn A (2010) Significance of long-chain polyunsaturated fatty acids (PUFAs) for the development and behaviour of children. Eur J Pediatr 169(2):149–164. https://doi.org/10.1007/s00431-009-1035-8
89. Collins MA (2015) Alcohol abuse and docosahexaenoic acid: effects on cerebral circulation and neurosurvival. Brain Circ 1(1):63–68. https://doi.org/10.4103/2394-8108.162533
90. Das UN (2006) Fetal alcohol syndrome and essential fatty acids. PLoS Med 3(5):e247. https://doi.org/10.1371/journal.pmed.0030247
91. Raabe RC, Mathies LD, Davies AG, Bettinger JC (2014) The omega-3 fatty acid eicosapentaenoic acid is required for normal alcohol response behaviors in C. elegans. PLoS One 9(8):e105999. https://doi.org/10.1371/journal.pone.0105999
92. Eberhart JK, Harris RA (2013) Understanding variability in ethanol teratogenicity. Proc Natl Acad Sci U S A 110(14):5285–5286. https://doi.org/10.1073/pnas.1302650110
93. Idrus NM, Thomas JD (2011) Fetal alcohol spectrum disorders: experimental treatments and strategies for intervention. Alcohol Res Health 34(1):76–85
94. Bearer CF (2001) L1 cell adhesion molecule signal cascades: targets for ethanol developmental neurotoxicity. Neurotoxicology 22(5):625–633. https://doi.org/10.1016/S0161-813X(01)00034-1
95. Guerri C, Bazinet A, Riley EP (2009) Foetal alcohol spectrum disorders and alterations in brain and behaviour. Alcohol 44(2):108–114. https://doi.org/10.1093/alcalc/agn105
96. Luo J (2012) Mechanisms of ethanol-induced death of cerebellar granule cells. Cerebellum 11(1):145–154. https://doi.org/10.1007/s12311-010-0219-0